# Non-Gaussian 1/*f* noise: Experimental optimization and separation of high-order amplitude and phase correlations

G. T. Seidler and S. A. Solin
*NEC Research Institute, 4 Independence Way, Princeton, New Jersey 08540*
(Received 13 November 1995)

The experimental optimization of the detection of non-Gaussian effects in resistance fluctuations was studied. Sensitivity-optimization criteria for the second spectrum, an important fourth-order statistical spectrum, were calculated and confirmed by experiment. Also, two additional fourth-order statistical spectra were introduced to separately and independently quantify the correlations in the amplitudes and in the phases of the Fourier coefficients of a noise signal. For a carbon resistor exhibiting non-Gaussian 1/*f* noise, the non-Gaussian effects were predominantly due to high-order phase correlations.

## I. INTRODUCTION

The study of the high-order statistics of the voltage noise of resistors has led to a number of important insights. These include the equilibrium nature of 1/*f* noise,[1,2] the hierarchical dynamics of the metastable states of metallic spin glasses,[3] the importance of the collective rearrangement of defects in the sliding state of charge-density waves,[4] and most recently, the presence of a plastic flow regime for the vortex lattice in clean superconductors.[5]

By definition, Gaussian noise is characterized as having both a Gaussian distribution function and also the property that all high-order statistics of Gaussian noise can be expressed in terms of second-order statistics, i.e., simple two-point correlation functions.[6] Thus, Gaussian noise is fully described by its histogram and power spectrum. When one studies higher-order statistics of random signals, i.e., order greater than two, the focus is to characterize and understand the non-Gaussian contributions to the fluctuations.

One of the important experimental measures of non-Gaussian resistance noise is the ''second spectrum'' introduced by Restle *et al.*[7] The second spectrum's utility rests in its sensitivity to weak correlations between noise-generating fluctuators. This utility is naturally constrained by both the experiment's overall sensitivity to non-Gaussian effects and also the level of detailed information which can be inferred from the resulting second spectrum. The purpose of this paper is correspondingly twofold. First, calculations and experiments are reported which aim at determining the experimental conditions necessary for optimal sensitivity to weak non-Gaussian effects in a noise signal. And second, two additional high-order statistic spectra are introduced for the study of non-Gaussian resistance fluctuations. Intimately related to the second spectrum, these two spectra separately probe, respectively, the correlations in the amplitudes and in the phases of the Fourier coefficients of the noise signal. As a test case, a carbon resistor exhibiting non-Gaussian 1/*f*-noise was studied. Surprisingly, the overwhelming contributor to non-Gaussianity was in the fourth-order phase correlations, with no statistically significant non-Gaussian signature in the amplitude correlations at the lowest frequencies probed by our experiments.

## II. COMPARISON OF EXPERIMENTAL SCHEMATA

The study of the high-order statistics of the voltage noise of resistors began with the conceptually important work of Voss and Clark.[1] To ascertain whether or not the 1/*f* noise observed from current-carrying resistors[8,9] is an equilibrium effect, they measured the power spectrum of the time-dependent variance of the Johnson noise. Their experiment is shown schematically in Fig. 1. The amplified $V(t)$ of the resistor is bandpass filtered, and then squared and averaged over an appropriate time constant by an analog squaring circuit and integrator to give the time-dependent variance of $V(t)$. This signal is read by an analog-to-digital converter (ADC), and finally the power spectrum of the variance is calculated using a fast Fourier transform (FFT). For a few resistors with large relative noise powers, they were able to observe a 1/*f* dependence in the power spectrum of the variance providing strong evidence that 1/*f* noise in current-carrying resistors is due to intrinsic resistance fluctuations.

A few years later, the commonly available computing power in condensed matter physics laboratories had ad-

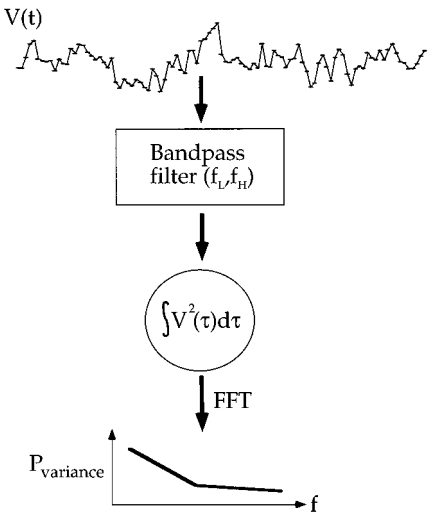


FIG. 1. The experimental configuration used by Voss and Clarke (Ref. 1) for measurement of the power spectrum of the variance of the Johnson noise power of resistors (see text for description).

 

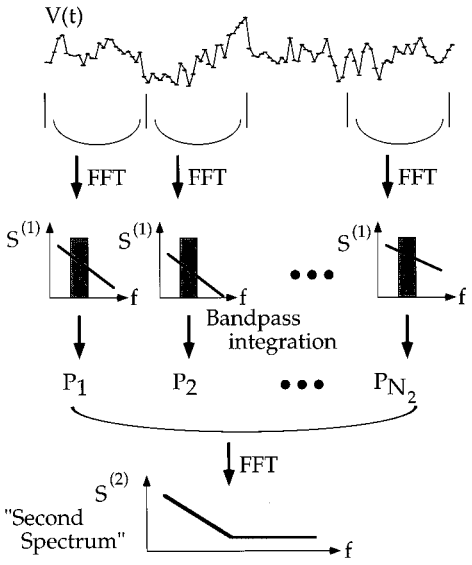


FIG. 2. The experimental configuration used by Restle *et al.* (Ref. 7) for measurement of a fourth-order statistic spectrum of $1/f$ noise (see text for description).

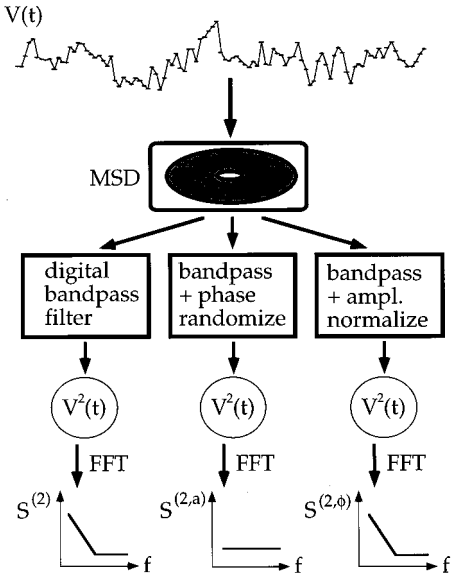


FIG. 3. A modification of the experimental configuration depicted in Fig. 2. The data $V(t)$ is stored on the mass storage device (MSD) and later digitally filtered to allow analysis of $V(t)$ in any bandpass (see text for complete description).

vanced considerably. To avoid the limitations imposed by data collection in any one particular bandpass and to remove any possible corruption of the noise signal by the analog squaring circuit, Restle *et al.*[7] introduced a somewhat different experimental configuration, which is depicted schematically in Fig. 2.

After appropriate amplification and anti-alias filtering, the time trace $V(t)$ is discretely sampled by an ADC and sequentially broken into $N_2$ contiguous segments of $N_1$ points. Let $f_s$ denote the sampling rate, $T_1=N_1/f_s$ the time duration of each data segment, and $T=N_2/f_s$ the total data collection time. The power spectrum is calculated using a FFT, and then integrated over a chosen bandpass to define a sequence of integrated noise powers $(P_i)$. As a consequence of Parseval's theorem,[6] $P_i$ is approximately equal to the output of the analog squaring and integration circuit element of Fig. 1 over the same time window and with the integration time set to $T_1$. Small differences in the two quantities are caused by differences in the roll-off of the analog bandpass in Fig. 1 and the effective roll-off imposed on filtering in Fourier space because of frequency bin smearing. Finally, the power spectrum of $P_i$ is calculated; this quantity has been intuitively named the second spectrum,[7] which is denoted here by $S^{(2)}$.

One motivating factor of the current paper is that the second spectrum contains information from both the fourth-order amplitude correlations and also the fourth-order phase correlations of the Fourier coefficients of $V(t)$. As the separation of the amplitude-correlation and phase-correlation contributors to $S^{(2)}$ may lead to further insight into the mechanisms underlying the various examples of non-Gaussian resistance fluctuations,[1–5,7] a third experimental configuration for the measurement of high order statistics of $V(t)$ is reported here. The techniques introduced here often require the FFT of data sets of $10^6$ points or more to extract useful information at the lowest experimentally accessible frequencies; such analysis can be completed on convenient time scales using present-day workstations or the fastest of the present-day personal computers. The modified experimental configuration is shown schematically in Fig. 3.

$V(t)$ is once again discretely sampled by an ADC after amplification and anti-alias filtering. These data are streamed to a mass storage device (MSD). Upon the completion of data collection several analyses are carried out. First, the data are digitally bandpass filtered, then squared point-by-point, and finally the power spectrum of the time-dependent variance of the noise signal is calculated. This computational path is the nearest digital equivalent of the experimental configuration of Fig. 1. Once again, the second spectrum obtained by this technique will differ slightly from those obtained by the previous two experiments only because of the details of the roll-offs of their respective bandpass filters.

The second analysis path in Fig. 3 is less conventional, but qualitatively similar to methods used in electron microscopy studies of amorphous materials.[10] Here, after applying a FFT to the data, a bandpass is imposed and the phases of the remaining nonzero Fourier coefficients are randomized. The resulting amplitude-sensitive second spectrum is denoted by $S^{(2,a)}$.

The final analysis quantifies the fourth-order phase correlations in the original signal. After taking the FFT of the data, a bandpass filter is again imposed but now the magnitude of each nonzero Fourier coefficient is set to unity, while leaving the phase unchanged; that is,

$$A_n=a_r\exp(i\phi_n)\rightarrow 1\exp(i\phi_n). \tag{1}$$

After performing the inverse FFT, the result of this nonlinear filter is bandpass-limited white noise containing exactly the phase correlations present in the original signal, but with all amplitude-dependent information obviously removed. In image processing this is known as ''whitening,'' and has been used to demonstrate the importance of phase

correlations in the information content of two-dimensional images.[11] We denote the resulting phase-sensitive second spectrum by $S^{(2,\phi)}$. Details on the implementation of each of these analyses follows below.

### III. GAUSSIAN BACKGROUND CALCULATIONS

The definitions of the second spectra introduced above will now be made rigorous, and several of their properties will be calculated. Consider a bandpass bounded above and below in frequency by $f_H$ and $f_L$, respectively, and define $b_H = Tf_H$ and $b_L = Tf_L$. We assume that $b_L > 0$. Following the general framework of Ref. 2, expansion of the bandpass limited $V(t)$ in a Fourier series yields

$$V(t) = \sum_{n=b_L}^{b_H} \{A_n \exp(2\pi i f_n t) + A_n^* \exp(-2\pi i f_n t)\} \quad (2)$$

so that

$$\begin{aligned} V^2(t) &= \sum_{m=b_L}^{b_H} \sum_{n=b_L}^{b_H} \{A_m A_n^* \exp[2\pi i (f_m - f_n)t] \\ &\quad + A_m A_n \exp[2\pi i (f_m + f_n)t] + \text{c.c.}\} \\ &= \sum_{p=0}^{\infty} \{C_p \exp(2\pi i f_p t) + C_p^* \exp(-2\pi i f_p t)\} \end{aligned} \quad (3)$$

with

$$\begin{aligned} C_p = \sum_{m=b_L}^{b_H} \sum_{n=b_L}^{b_H} \{&A_m A_n \delta_{p,m+n} + A_m A_n^* \delta_{p,m-n} \\ &+ A_m^* A_n (\delta_{p,n-m} - \delta_{p,0}\delta_{m,n})\}. \end{aligned} \quad (4)$$

Individual Fourier coefficients of $V^2(t)$ consist of the superposition of all beats of appropriately related frequencies present in the bandpass limited signal $V(t)$; the first term in Eq. (4) is the contribution from sum-beats, the last two terms from difference-beats with $m \geq n$ and $m < n$, respectively. The second spectrum is given by

$$\begin{aligned} S_p^{(2)} = 2TC_p C_p^* = 2T \sum_{j=b_L}^{b_H} \sum_{k=b_L}^{b_H} \sum_{m=b_L}^{b_H} \sum_{n=b_L}^{b_H} &\{A_j A_k \delta_{p,j+k} \\ &+ A_j A_k^* \delta_{p,j-k} + A_j^* A_k \delta_{p,k-j}\}\{A_m^* A_n^* \delta_{p,m+n} \\ &+ A_m^* A_n \delta_{p,m-n} + A_m A_n^* \delta_{p,n-m}\} \end{aligned} \quad (5a)$$

for $p > 0$ and

$$S_0^2 = 4T \left( \sum_{m=b_L}^{b_H} A_m A_m^* \right)^2 \quad (5b)$$

for $p = 0$; henceforth we assume that $p > 0$. This is the key point where the assumption of Gaussian noise is to be made, or alternatively, where the necessary characteristics for possible contributions from non-Gaussian noise are to be examined.

Given that the existing literature on $S^{(2)}$ always demonstrates non-Gaussian phenomenon only in the low beat-frequency limit,[3,7,9] the present discussion is restricted to $f_p < 2f_L$ and hence ignores the terms in Eq. (5a) coming from sum-beats. Equation (5a) then simplifies after contracting two pairs of summations with the $\delta$ functions and relabeling the indices, giving

$$\langle S_p^{(2)} \rangle = 8T \sum_{k=b_L}^{b_H-p} \sum_{n=b_L}^{b_H-p} \langle A_{k+p} A_k^* A_{n+p}^* A_n \rangle. \quad (6)$$

If the fluctuations in $V(t)$ are Gaussian, then

$$\begin{aligned} \langle S_p^{(2)} \rangle_{\text{Gaussian}} &= 8T \sum_{n=b_L}^{b_H-p} \langle A_{n+p} A_{n+p}^* \rangle \langle A_n A_n^* \rangle \\ &= \frac{2}{T} \sum_{n=b_L}^{b_H-p} \langle S_{n+p}^{(1)} \rangle \langle S_n^{(1)} \rangle. \end{aligned} \quad (7)$$

The equation defines the so-called Gaussian background of $S^{(2)}$. As pointed out by Beck and Spruit[2] in the context of non-Gaussian Johnson noise,[1] this background is a direct consequence of the finite detection bandwidth of the measurement.

To determine the Gaussian backgrounds in $S^{(2,a)}$ and $S^{(2,\phi)}$, rewrite Eq. (6) in polar coordinates,

$$\begin{aligned} \langle S_p^{(2)} \rangle = 8T \sum_{k=b_L}^{b_H-p} \sum_{n=b_L}^{b_H-p} \langle a_{k+p} a_k a_{n+p} a_n \exp\{i[(&\phi_{k+p} \\ &- \phi_k) - (\phi_{n+p} - \phi_n)]\} \rangle. \end{aligned} \quad (8)$$

If the phase differences are uncorrelated then only those terms with $n = k$ will have nonzero expectation and contribute to the sum. Therefore

$$\langle S_p^{(2a)} \rangle = 8T \sum_{n=b_L}^{b_H-p} \langle A_{n+p} A_{n+p}^* A_n A_n^* \rangle = \frac{2}{T} \sum_{n=b_L}^{b_H-p} \langle S_{n+p}^{(1)} S_n^{(1)} \rangle. \quad (9)$$

In the limit of Gaussian noise, this reduces to Eq. (7); the Gaussian backgrounds of $S^{(2)}$ and $S^{(2,a)}$ are identical.

Returning to Eq. (8), it follows from the definition of $S^{(2,\phi)}$ that

$$\begin{aligned} \langle S_p^{(2,\phi)} \rangle = 8T \sum_{k=b_L}^{b_H-p} \sum_{n=b_L}^{b_H-p} \langle \exp\{i[(&\phi_{k+p} - \phi_k) \\ &- (\phi_{n+p} - \phi_n)]\} \rangle. \end{aligned} \quad (10)$$

As a consequence of the sums having the same bounds, it is not difficult to show that

$$\begin{aligned} \langle S_p^{(2,\phi)} \rangle = 8T \sum_{k=b_L}^{b_H-p} \sum_{n=b_L}^{b_H-p} \langle \cos[(&\phi_{k+p} - \phi_k) \\ &- (\phi_{n+p} - \phi_n)] \rangle. \end{aligned} \quad (11)$$

In the limit of Gaussian noise, once again only terms with $n = k$ have nonzero expectation, and thus

$$\langle S_p^{(2,\phi)} \rangle_{\text{Gaussian}} = 8T(b_H - b_L - p) = 8T^2(f_H - f_L - f_p). \quad (12)$$

The normalized second spectra are defined by

$$s_p^{(2)}=\frac{S_p^{(2)}}{\left\langle \frac{1}{T}\sum_{n=b_L}^{b_H} S_n^{(1)} \right\rangle^2}, \tag{13a}$$

$$s_p^{(2,a)}=\frac{S_p^{(2a)}}{\left\langle \frac{1}{T}\sum_{n=b_L}^{b_H} S_n^{(1)} \right\rangle^2}, \tag{13b}$$

and

$$s_P^{(2,\phi)}=\frac{S_p{}^{(2,\alpha)}}{4T^2(f_H-f_L)^2}. \tag{13c}$$

The normalized second spectra each have units of $\mathrm{Hz}^{-1}$. A similar normalization in the definition of the second spectrum has been used in previous works employing the experimental configuration of Fig. 2.[3]

As a consequence of the whitening imposed on the data in the definition of $S^{(2,\phi)}$, it follows that

$$\langle s_p^{(2,\phi)}\rangle_{\text{Gaussian}}=\frac{2(f_H-f_L-f_p)}{(f_H-f_L)^2} \tag{14}$$

for any broadband example of $S^{(1)}$, whether white, $1/f$, Lorentzian, or more complicated.

Using Eq. (7) and the above definitions, the Gaussian backgrounds of the normalized second spectrum $s^{(2)}$ can now be calculated for several physically relevant examples of $S^{(1)}$. First, consider Johnson noise, which has

$$\langle A_n A_n^*\rangle=2k\theta R/T, \tag{15}$$

where $k$ is Boltzmann's constant, $\theta$ is the temperature, and $T$ is the total measurement time. One obtains

$$\langle s_p^{(2)}\rangle_{\text{Johnson}}=\frac{\langle S_p^{(2)}\rangle}{\left\langle \frac{1}{T}\sum_{n=b_L}^{b_H} S_n^{(1)} \right\rangle^2}=\frac{2(f_H-f_L-f_p)}{(f_H-f_L)^2} \tag{16}$$

as should be expected from the above discussion of the Gaussian background of $s^{(2,\phi)}$ because Eq. (15) is white. [In general, the Gaussian backgrounds of $s^{(2)}$ and $s^{(2,\phi)}$ are quite different, as is demonstrated below.] In the low-$f_p$ limit Eq. (16) differs by a factor of two from that of Beck and Spruit.[2] comparison to experiment is presented below.

Pure $1/f$ noise also allows a simple evaluation of the Gaussian background. After replacing the pertinent sums by the corresponding integrals in Eq. (13a) it really follows that

$$\langle s_p^{(2)}\rangle_{\text{Gaussian}}=\frac{2}{f_P}\frac{\ln[(f_H-f_p)(f_L+f_p)/f_H f_L]}{[\ln(f_H/f_L)]^2} \tag{17}$$

and

$$\lim_{p\to 0}\langle s_p^{(2)}\rangle_{\text{Gaussian}}=\frac{2(f_H-f_L)}{f_H f_L[\ln(f_H f_L)]^2}. \tag{18}$$

Extremizing with respect to $f_L$ at fixed $f_H$ yields a local minimum in the low-$f_p$ Gaussian background when $f_H/f_L\approx 4.921$. Hence

$$\min(\lim_{p\to 0}\langle s_p^{(2)}\rangle_{\text{Gaussian}})=\left.\frac{2(f_H-f_L)}{f_H f_L[\ln(f_H/f_L)]^2}\right|_{f_H/f_L=4.921}$$

$$\approx\frac{3.088}{f_H}. \tag{19}$$

The common practice of taking octave-sized bandpasses[3,7] is therefore suboptimal for detection of weak non-Gaussian signatures in $V(t)$. Also, one can see from Eq. (19) that the Gaussian background decreases with increasing $f_H$. Both of these features are verified by experiments described below in the current paper. Unfortunately, the general case of a power law noise power does not lend itself to a closed solution of the resulting integrals; instead the Gaussian backgrounds must be calculated numerically from Eqs. (7) and (13a).

Finally, for completeness, consider the case when $S^{(1)}$ is Lorentzian with zero center frequency,

$$\langle A_n A_n^*\rangle=\frac{\alpha}{(1+n^2/T^2 f_0^2)}, \tag{20}$$

where $f_0$ is the knee frequency. Such a first spectrum occurs, for example, in the important case of a two-level system,[8,9] and also in experiments of the type of Voss and Clarke[1,2] where $f_0$ would be the rc frequency of the combined sample resistance and circuit stray capacitance. Then

$$\langle s_p^{(2)}\rangle_{\text{Gaussian}}=\frac{8T^2\alpha^2\int_{f_L}^{f_H-f_P} df/[(1+f^2/f_0^2)\{1+(f+f_p)^2/f_0^2\}]}{\left\{2T\alpha\int_{f_L}^{f_H}\frac{df}{(1+f^2/f_0^2)}\right\}^2}$$

$$=\frac{2}{f_0}\frac{\left[\frac{f_0}{f_p}\ln\left(\frac{1+(f+f_p)^2/f_0^2}{1+(f/f_0)^2}\right)+\arctan(f/f_0)+\arctan[(f+f_p)/f_0]\right]\Big|_{f_L}^{f_H-f_p}}{[4+(f_p/f_0)^2][\arctan(f_H/f_0)-\arctan(f_L/f_0)]^2}. \tag{21}$$

## IV. EXPERIMENT

The resistances of the samples studied here fall within the narrow range from 1 – 2 kΩ. The same amplifier and filter chain therefore could be and in fact was used for all measurements of the second spectra. Specifically, the first preamplifier was a Stanford Research model 552 bipolar transistor amplifier. The boost amplifier was a Princeton Applied Research model 113. A Stanford Research model 640 was used as a low-pass filter for anti-aliasing and, in some cases, for additional gain. The SR552 was verified to have a noise figure of less than 3 dB for all samples reported here. In the studies of 1/$f$ noise, the power supply was a series chain of four 12.5 V Panasonic batteries with either a commercial metal-film resistor or a Genrad 1433-G wirewound-resistance decade box as the current limiting resistor. Measurements of the first spectra were obtained either using standard dc techniques with the above apparatus, or by a standard ac technique[12] for frequencies below 1 Hz. All data were collected at room temperatures in a temperature and humidity controlled room, with the sample, the batteries, and the first two amplifiers in magnetically shielded, draft-free environments.

Effective 14-bit analog-to-digital conversion was obtained from a National Instruments MIO-16X general purpose peripheral board in a 66 MHz 80486 PC. Some real-time analysis of $s^{(1)}$ and $s^{(2)}$ was performed by the data collection PC, but all computations presented here were performed on a multi-R8000-processor workstation equipped with 1 Gbyte of RAM; the large RAM was more than sufficient to allow the most computationally demanding FFT's necessary for the present experiments (8 Mpoints) to be performed without the use of virtual memory via disk swapping. The **real ft**( ) and **four1**( ) routines from Numerical Recipes[13] were used in our C-language analysis software.

## V. RESULTS AND DISCUSSION

First $s^{(2)}$ for the Johnson noise of a commercial 2.00 kΩ metal-film resistor at room temperature was measured. The power spectrum was indeed found to be white (not shown), and the noise figure of the preamplifier was less than 0.5 dB. The second spectrum was also found to be white at low frequencies, as shown in Fig. 4 for various bandpasses. The solid curves in the figure are graphs of Eq. (16) with no free parameters. The calculation is in excellent agreement with the data.

Next, a simple experiment was performed which serves two roles. First, agreement with the calculations of the Gaussian background for 1/$f$ noise was demonstrated. Second, it was proven that the chosen normalization for $s^{(2)}$ is in fact a relevant choice for questions of detectability of weak non-Gaussian effects.

The sample was a manually deposited carbon-composite resistor with dimensions ~0.2 mm long ×1.0 mm wide ×1 μm thick and $R=1.61$ kΩ;[14] copper leads were attached in a quasi-four-probe configuration with silver paint. The power spectrum was found to scale roughly as $1/f^{1.15}$ from 10 mHz to 12 kHz as shown in Fig. 5. In Fig. 6, $s^{(2)}$ is shown for three different bandpasses with $I=47$ μA and the data set consisting of $N=8$ Mpoints continuous measurements at a sampling rate of 30 kHz. The roll-off of the anti-aliasing filter was set at 13 kHz. The three bandpasses are concentric about $f=7.2$ kHz, i.e., $(f_L, f_H)=$(7.05 kHz, 7.35 kHz) open circles, (6.6 kHz, 7.8 kHz) open triangles, (4.8 kHz, 9.6 kHz) filled circles. The dashed lines are the prediction of Eq. (17) for the Gaussian backgrounds of the three bandpasses.

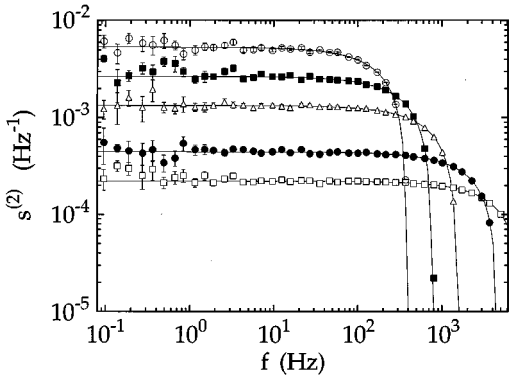


FIG. 4. The second spectrum $s^{(2)}$ for Johnson noise from a 2.00 kOhm resistor at room temperature for various bandpasses. The sampling frequency was 30 kHz, and $N=8$ Mpoints. From top to bottom in the figure the bandpass limits are $(f_L, f_H)=$(4.5 kHz, 4.875 kHz), (9 kHz, 9.75 kHz), (1.5 kHz, 3 kHz), (3 kHz, 7.5 kHz), (3 kHz, 12 kHz). The solid lines are plots of Eq. (16) for each of the specified bandpasses.

At the lowest frequencies depicted in the figure, i.e., where the signal-to-background ratio is large, the three spectra agree well. Further, the threshold frequency where deviations from the predicted Gaussian backgrounds occur systematically increase as the Gaussian background is lowered. As these bandpasses are concentric and fairly narrow, the resulting $s^{(2)}$ necessarily characterize the same non-Gaussian effects.[9] The choice of normalization for $s^{(2)}$ made in Eq. (13) is verified to be valid for questions of detectability; i.e., a lower Gaussian background in $s^{(2)}$ does in fact imply a more sensitive measurement.

In Fig. 7, $s^{(2)}$ is evaluated at $f=100$ Hz for a number of different bandpasses all with $f_H=12$ kHz. Note the local minimum at $f_H/f_L\sim 5$, as predicted by Eq. (19). The dashed line in the figure is the prediction of Eq. (17) for $f_p=100$ Hz. The deviation is consistent with some residual non-Gaussianity at these frequencies.

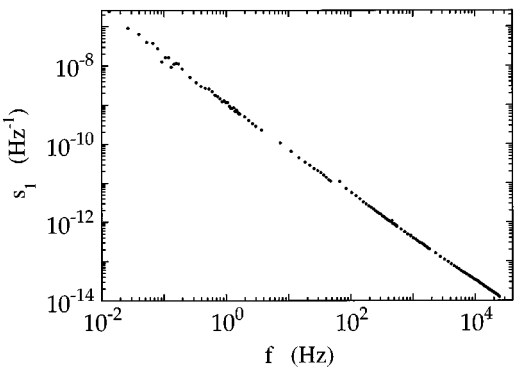


FIG. 5. The normalized first spectrum $S^{(1)}$ corrected for Johnson noise for the homemade carbon resistor described in the text.

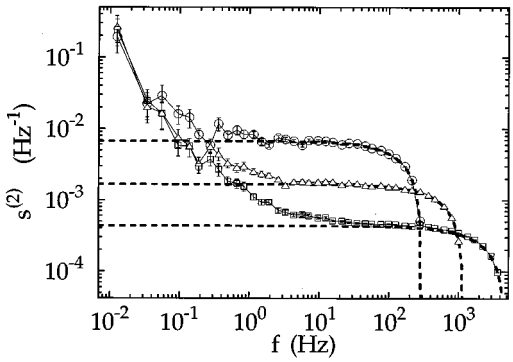


FIG. 6. $s^{(2)}$ for the homemade carbon composite resistor described in the text at room temperture with $I=47$ $\mu$A and $N=8$ Mpoints. $s^{(2)}$ is shown for three progressively wider bandpasses, each concentric about $f=7.2$ kHz. $(f_L, f_H)$ = (7.05 kHz, 7.35 kHz) open circles, (6.6 kHz, 7.8 kHz) open triangles, (4.8 kHz, 9.6 kHz) filled circles. The dashed lines are the prediction of Eq. (17) for the Gaussian backgrounds of the three bandpasses. Note the systematic improvement in detectability of non-Gaussian effects with increasing bandwidth.

One can of course instead hold $f_H/f_L$ constant while varying the bandpass limits. In Fig. 8, $s^{(2)}$ is again evaluated at 100 Hz for the same data set but now as a function of $f_H$ with $f_H/f_L$ held equal to 5. The dashed line is the prediction of Eq. (17) with $f_p=100$ Hz. As was the case with Fig. 7, the data shows a small systematic deviation from the calculated background for perfect $1/f$ noise.

Despite the small differences between the experiments and the calculations, it is clear that the Gaussian background has a local minimum as a function of $f_H/f_L$ and decreases monotonically with increasing $f_H$. In those cases where non-Gaussianity exists at high frequencies, it is the combination of the latter property with the desire to probe $s^{(2)}$ over the widest possible beat-frequency range that necessitates the use of large data sets.

Finally, the family of second spectra for the sample and data set analyzed in the preceding four figures is presented in Fig. 9. The solid curve is the predicted Gaussian background for $s^{(2)}$ (and also for $s^{(2,a)}$) from Eq. (17) assuming a perfect $1/f$ power spectrum. The dashed line in the figure shows the

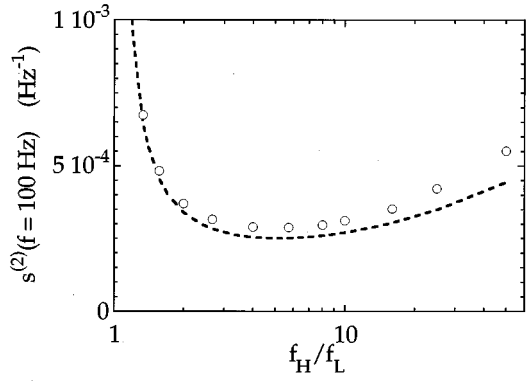


FIG. 7. The open circles are $s^{(2)}$ evaluated at $f=100$ Hz for the same data set as was studied in Fig. 5 with $f_H=12$ kHz for all bandpasses. The dashed line is the prediction of Eq. (17) with $f_p=100$ Hz.

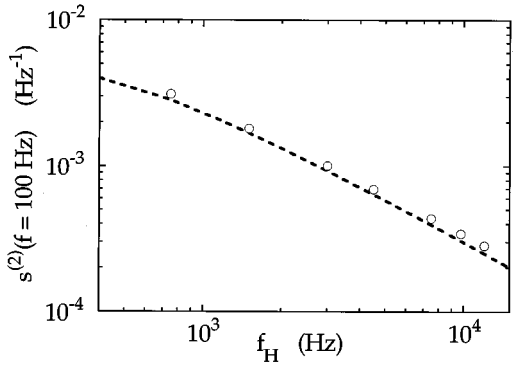


FIG. 8. The open circles are $s^{(2)}$ evaluated at $f=100$ Hz for the same data set as was studied in Fig. 5 with $f_H/f_L=5$ for all bandpasses. The dashed line is the prediction of Eq. (17) with $f_p=100$ Hz.

Gaussian background for $s^{(2,\phi)}$, as per Eq. (14).

One subtlety special to the computation of $s^{(2,\phi)}$ exists: it is necessary to use a simple square window on the initial FFT of $V(t)$. Smoother windows insert unacceptable levels of spurious phase correlations into the data. This technique (with the square window) was tested on an extensive variety of data with known absence or presence of fourth-order phase correlations, including: real Johnson noise, Gaussian $1/f$ noise generated by power-law filtering of real Johnson noise, artificially generated Gaussian noise with a variety of physically relevant noise-power spectra, and various artificially generated non-Gaussian signals. In all tests no spurious correlations were introduced when a simple square window was used on the data FFT. However, the use of a square window has the drawback of frequency smearing in the power spectrum which decreases only as $1/(\Delta f)^2$,[13] which may severely limit the usefulness of this technique when studying narrow-band noise signals.

Returning to Fig. 9, note the similarity between the behaviors of $s^{(2)}$ and $s^{(2,\phi)}$. Furthermore, note the absence of statistically significant non-Gaussian behavior in $s^{(2,a)}$. The

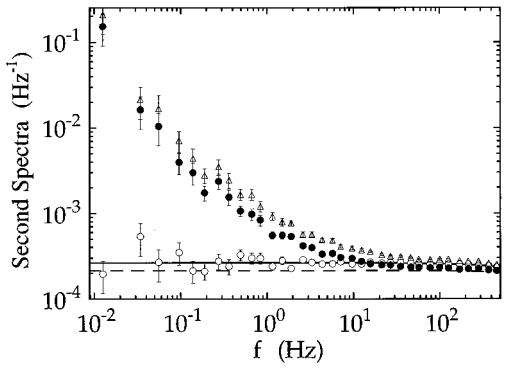


FIG. 9. The second spectra for the carbon resistor studied in the preceding figures for the bandpass (2.34 kHz, 11.7 kHz). The open triangles are $s^{(2)}$, the filled circles are $s^{(2,\phi)}$, and the open circles are $s^{(2,a)}$. The solid line is the prediction of Eq. (17) for the Gaussian background of $s^{(2)}$ and $s^{(2,a)}$ for perfect $1/f$ noise in the chosen bandpass. Similarly, the dashed line is the prediction of Eq. (14) for the Gaussian background of $s^{(2,\phi)}$.

importance of phase information has been recognized in the analysis of scattering experiments,[15] in the reconstruction of two-dimensional (2D) pictures from their Fourier coefficients,[11] and in the intelligibility of human speech.[11] To the best of our knowledge, this is the first demonstration of the predominance of phase information for non-Gaussian 1/$f$ noise. Preliminary results of an ongoing study of 1/$f$ noise in GaAs/$Al_xGa_{1-x}As$ superlattices[16] also demonstrate statistically significant non-Gaussian behavior only as a consequence of fourth-order phase correlations. A more complete discussion of this phenomenon, including extensive computer simulations of typical physical fluctuators, is in progress and will be reported elsewhere.[17]

## VI. CONCLUSIONS

In summary, optimization criteria for the detection of weak non-Gaussian effects in resistance noise were calculated and verified by experiment. Also, borrowing nonlinear filters which have been used with success in 2D image processing,[10,11] two additional second spectra were introduced for the study of resistance fluctuations. Unlike the original method of Restle *et al.*,[7] the new spectra allow precise separation of the high-order correlations in the amplitudes and in the phases of the Fourier coefficients of a noise signal. Non-Gaussian 1/$f$ noise from a carbon resistor displayed statistically significant non-Gaussian fluctuations only as a consequence of high-order phase correlations.

## ACKNOWLEDGMENTS

We thank S. Bhattacharya, W. Bialek, R. de Ruyter, and M. Treacy for useful discussions during the preparation of this manuscript.

[1] Richard F. Voss and John Clarke, Phys. Rev. B **13**, 556 (1976).
[2] H.G.E. Beck and W.P. Spruitt, J. Appl. Phys. **49**, 3384 (1978).
[3] N.E. Israeloff, G.B. Alers, and M.B. Weissman, Phys. Rev. B **44**, 12 613 (1991); M.B. Weissman, N.E. Israeloff, and G.B. Alers, J. Magn. Magn. Mater. **114**, 87 (1992); M.B. Weissman, Rev. Mod. Phys. **65**, 829 (1994).
[4] I. Bloom, A.C. Marley, and M.B. Weissman, Phys. Rev. Lett. **71**, 4385 (1993); I. Bloom, A.C. Marley, and M.B. Weissman, Phys. Rev. B **50**, 5081 (1994).
[5] A.C. Marley, M.J. Higgins, and S. Bhattacharya, Phys. Rev. Lett. **74**, 3029 (1995).
[6] Julias S. Bendat and Allan G. Piersol, *Random Data: Analysis and Measurement Procedures*, 2nd ed. (Wiley, New York, 1986).
[7] P.J. Restle, R. J. Hamilton, M.B. Weissman, and M.S. Love, Phys. Rev. B **31**, 2254 (1985).
[8] P. Dutta and P.M. Horn, Rev. Mod. Phys. **53**, 497 (1981).
[9] M.B. Weissman, Rev. Mod. Phys. **60**, 537 (1988).
[10] O.L. Krivanek, P.H. Gaskell, and A. Howie, Nature **262**, 454 (1975); G.Y. Fan and J.M. Crowley, Ultramicroscopy **24**, 49 (1988).
[11] Alan V. Oppenheim and Jae S. Lim, Proc. IEEE **69**, 529 (1981), and references therein.
[12] John H. Scofield, Rev. Sci. Instrum. **58**, 985 (1987).
[13] William H. Press, Brian P. Flannery, Saul A. Teukolsky, and William T. Vetterling, *Numerical Recipes in C: The Art of Scientific Computing* (Cambridge University Press, Cambridge, 1988).
[14] Carbon source: DIXON Oriole #287, 2/HB.
[15] G.N. Ramachandran and R. Srinivasan, Nature **190**, 159 (1961).
[16] G.T. Seidler, S.A. Solin, and A.C. Marley (unpublished).
[17] G.T. Seidler and S.A. Solin (unpublished).